Multiorder nonlinear diffraction in frequency doubling processes

Solomon M. Saltiel,[1,2,*] Dragomir N. Neshev,[1] Wieslaw Krolikowski,[1] Ady Arie,[3] Ole Bang,[4] and Yuri S. Kivshar[1]

[1]*Nonlinear Physics Centre and Laser Physics Centre, Centre for Ultra-high Bandwidth Devices for Optical Systems (CUDOS), Research School of Physics and Engineering, The Australian National University, Canberra ACT 0200, Australia*

[2]*Department of Quantum Electronics, Faculty of Physics, Sofia University, BG-1164 Sofia, Bulgaria*

[3]*School of Electrical Engineering, Tel-Aviv University, Tel Aviv 69978, Israel*

[4]*Department of Photonics Engineering, DTU Fotonik, Technical University of Denmark, DK-2800 Kongens Lyngby, Denmark*

**Corresponding author: saltiel@phys.uni-sofia.bg*

Received December 8, 2008; revised January 22, 2009; accepted January 30, 2009; posted February 27, 2009 (Doc. ID 105073); published March 13, 2009

We analyze experimentally light scattering from $\chi^{(2)}$ nonlinear gratings and observe two types of second-harmonic frequency-scattering processes. The first process is identified as Raman–Nath type nonlinear diffraction that is explained by applying only transverse phase-matching conditions. The angular position of this type of diffraction is defined by the ratio of the second-harmonic wavelength and the grating period. In contrast, the second type of nonlinear scattering process is explained by the longitudinal phase matching only, being insensitive to the nonlinear grating period. © 2009 Optical Society of America

OCIS codes: 190.4420, 190.2620, 050.1940.

Second-harmonic generation (SHG) is one of the most studied parametric processes in nonlinear optics. Often, to achieve efficient SHG, this process requires periodic modulation of the $\chi^{(2)}$ components, the so-called quasi-phase-matching (QPM) [1]. Usually, QPM is realized by collinear propagation of the fundamental frequency (FF) and second-harmonic (SH) beams along the QPM grating vector. However, when the FF beam and the QPM grating vector are noncollinear, then the SH beam diffracts from the $\chi^{(2)}$ grating in a fashion similar to a linear beam diffraction on an index grating.

In the linear optics it is well established that propagation of a light beam in periodic refractive index structures leads either to *Bragg diffraction* when the full vectorial phase-matching condition is satisfied or to *Raman–Nath diffraction* otherwise [2]. In the latter case since the full vectorial phase matching is not fulfilled, a multiorder diffraction takes place, similar to the case of light scattering by acoustic waves.

Analogously, nonlinear Bragg diffraction is realized at a specific angle between the beams [3], determined by the vectorial phase matching $2\mathbf{k_1}+\mathbf{G_n}=\mathbf{k_2}$, where $\mathbf{G_n}$ is the grating vector and $\mathbf{k_1}$, $\mathbf{k_2}$ are the wave vectors of the FF and SH beams, respectively [Fig. 1(a)]. If this vectorial condition is not satisfied, multiorder nonlinear SH diffraction should be seen, in an analog to linear Raman–Nath diffraction [Fig. 1(b)].

Nonlinear Bragg diffraction has been observed in a number of structures, including naturally laminated crystals [3–5], as well as artificially created nonlinear one-dimensional [6–9] and annular [10] $\chi^{(2)}$ gratings. On the other hand, to the best of our knowledge, the nonlinear Raman–Nath diffraction has not been discussed so far, simply because QPM technology is mainly used for photonics components with collinear propagation. In fact, the first experimental indication of this phenomena has been reported in our recent work [10], where the first- and second-order nonlinear diffraction in annular QPM structure was observed.

In this Letter we study the nonlinear diffraction of beams from a one-dimensional nonlinear grating, realized by periodic spatial alternation of the sign of the relevant components of the $\chi^{(2)}$ tensor. We observe multiple-order nonlinear diffraction in the SHG processes, which represents the Raman–Nath contribution to the process. In addition, we analyze the diffracted SH beams that are governed only by longitudinal phase-matching conditions and can be classified as noninteger order nonlinear diffraction, having no analog in linear optics.

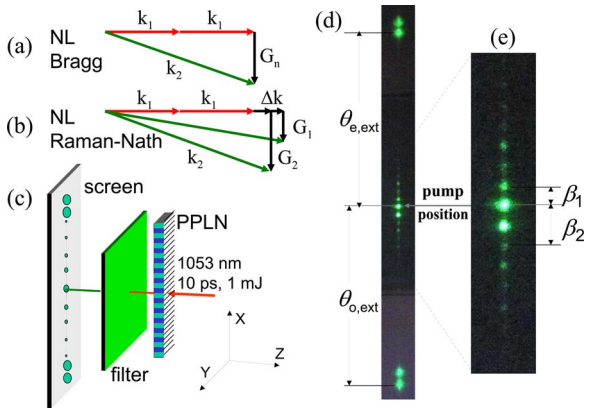

Fig. 1. (Color online) Phase-matching conditions for (a) nonlinear Bragg and (b) Raman–Nath diffraction. (c) Schematic of the experiment. (d), (e) Experimentally observed nonlinear diffraction patterns generated in one-dimensional QPM grating in PPLN with period $\Lambda = 14.6\ \mu$m.

0146-9592/09/060848-3/$15.00

In our experiments we use periodically poled lithium niobate (PPLN) and stoichiometric lithium tantalate (SLT) samples (typical thickness 0.5 mm) in the arrangement shown in Fig. 1(c). The fundamental pump beam from a regenerative amplifier, delivering 10 ps, 1 mJ pulses at 1053 nm with repetition rate of 20 Hz, is directed at a small angle with respect to the Z axis. The laser beam is focused with a lens creating a spot size of $\approx$400 μm in the plane of the crystal.

In Figs. 1(d) and 1(e) we show an example of the SH diffraction patterns obtained in one-dimensional $\chi^{(2)}$ grating ($\Lambda = 14.6$ μm) in PPLN. The patterns consist of two types of spots: (i) central diffraction spots, grouped around the pump position, and (ii) peripheral diffraction spots, situated relatively far from the pump at both sides of the diffraction array [top and bottom pairs in Fig. 1(d)]. The two neighboring peripheral spots at each side of the array are orthogonally polarized. The spots that are furthest away from the pump are polarized in the $x-y$ plane, the other spots are polarized in the $x-z$ plane. Since the pump is ordinary polarized, we identify the interactions that are responsible for these SH spots as $O_2-O_1O_1$ and $E_2-O_1O_1$, respectively. The PPLN $\chi^{(2)}$ components that contribute to the $O_2-O_1O_1$ process are d_{22} and d_{21}, while for the $E_2-O_1O_1$ interaction the second-order polarization term involves additionally both d_{32} and d_{31} components. Similar $O_2-O_1O_1$ spots have been observed recently in periodically poled KTP [11], however, in contrast to our experiments, they were due to second-order nonlinearities existing only in the domain walls.

The observed nonlinear diffraction patterns can be explained by employing the phase-matching conditions shown in Fig. 2. The general vectorial phase-matching condition $\mathbf{2k_1}+\mathbf{G_n}+\mathbf{\Delta k}=\mathbf{k_2}$ is valid for both types of the SHG diffraction spots (the central and peripheral ones). Figure 2 shows one of the phase-matching triangles (OCD) that governs the first-order SH diffraction patterns, appearing close to the pump. It is constructed by the vectors $\mathbf{k}_{2,o}$, $2\mathbf{k}_{1,o}$, BD$=\mathbf{\Delta k}_{\mathrm{TPM}}$, and one of the grating vectors $\mathbf{G_o}$. The angular direction of the SH diffraction spot is defined only by the transverse phase-matching (TPM) conditions: $\sin\alpha_m = mG_o/k_{2,o}$, for the mth diffraction order, $m = 1,2,3\ldots$. The external angles then are

$$\sin\beta_m = m\lambda_2/\Lambda, \quad m = 1,2,\ldots, \tag{1}$$

where λ_2 is the SH wavelength. This is a generic condition that holds for any periodically poled sample and does not depend on its refractive index. Our measurements of the first-order SH diffraction angles for four (PPLN and SLT) samples with different grating periods (7.5, 9.0, 14.6, 24.1 μm) are shown in Fig. 3(a). The experimentally measured angles are in excellent agreement with the predictions of Eq. (1). We note that Eq. (1) is known to describe normal incidence Raman–Nath diffraction in linear optics.

For normal pump incidence, $\alpha_{-m} = -\alpha_{+m}$. For the pump incident at the angle γ with respect to the Z axis toward the X axis (in the plane X–Z), again we have $\alpha_{-m}(\gamma) = -\alpha_{+m}(\gamma)$ but the angles are defined by $\sin\alpha_m(\gamma) = (mG_o/k_{2,o})\cos\gamma$, derived again using the TPM condition only. Calculating the external angles gives that $\beta_m(\gamma) > \beta_m(\gamma=0)$. The dependence $\beta_m(\gamma)$ has been verified experimentally and the result is shown in Fig. 3(b).

In summary, so far we have demonstrated that the observed central SH multiorder diffraction [Fig. 1(e)] is a nonlinear optical analog of Raman–Nath diffraction. In this process, the directions of the SH diffracted beams can be determined by applying the TPM conditions only.

Next, we describe the phase-matching conditions for the peripheral SH spots that appear far from the pump. Experiments with four different samples show that their angular positions, θ_o and θ_e [defined in Figs. 1(d) and 2], do not depend on the poling period. This is in strong contrast to the direct angular dependence of the central diffraction spots on Λ, as seen from Eq. (1). The measured angles can be explained only if we assume that the directions of these SH beams are defined uniquely by the longitudinal phase-matching (LPM) condition, seen as the triangle OAB in Fig. 2, constructed by the vectors $\mathbf{k}_{2,e}$, $2\mathbf{k}_{1,o}$, $FA = \mathbf{\Delta k}_{\mathrm{LPM}}$, and m grating vectors, $BF = m\mathbf{G_o}$. Correspondingly, the phase-matching triangle for the ordinary SH wave is OBG.

For normal incidence, the measured angles θ_o and θ_e are found to be in accordance with those derived on the basis of LPM equations,

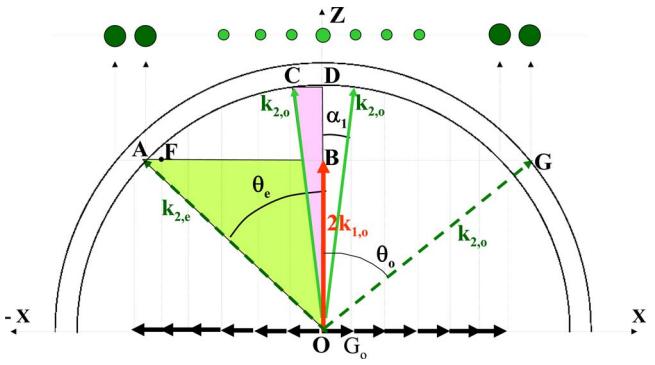

Fig. 2. (Color online) Phase-matching diagrams for SH diffraction when pump is perpendicular to the QPM grating. The two semicircles correspond to the ordinary and extraordinary wave vectors.

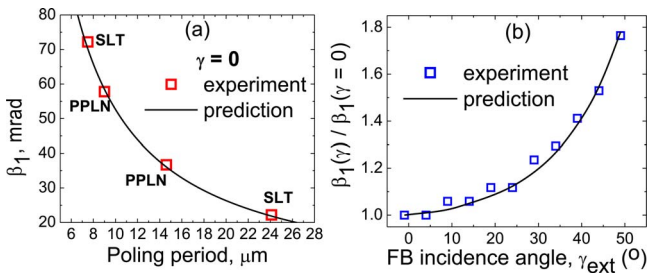

Fig. 3. (Color online) (a) External angle of first-order TPM-SH in four samples with different grating periods. (b) Increase of the first-order TPM-SH external angle with the angle of FF beam incidence for a PPLN sample ($\Lambda = 14.6$ μm).

$$\cos\theta_e = 2k_{1,o}/k_{2,e}(\theta_e), \quad \cos\theta_o = 2k_{1,o}/k_{2,o}. \qquad (2)$$

These equations are also known to define the emission of Cherenkov SH generation [12] and noncollinear SHG in one- and two-dimensional random nonlinear gratings [13–15]. In the PPLN crystal $n_o > n_e$, so that $|\theta_o| > |\theta_e|$. The angles measured for O_2–O_1O_1 and E_2–O_1O_1 interactions are 40.3° and 38.4°, in good agreement with theory at 1.053 μm, giving values of 40.64° and 38.78°, respectively.

For the pump propagating at an angle γ with respect to the Z axis [see inset in Fig. 4(b)], the phase matching for the LPM diffraction spots is obtained from Eq. (2) by replacing $2k_1$ with $2k_1 \cos\gamma$. An increase of the angle γ thus leads to an increase in both $|\theta_o|$ and $|\theta_e|$. We should mention that the angular positions θ_o and θ_e are determined from the direction of the Z axis, so that increasing the angle γ leads to a reduction of the angle between the pump and one of the diffraction spots. This is illustrated by an additional experiment where the SH pattern is recorded as a function of the crystal rotation around the Y axis. The recorded images are shown in Fig. 4(a). With the increase of the angle γ_{ext}, the phase-matching angles for both interactions increase. As seen from Fig. 4, the angle $\theta_{o,e,\text{ext}} - \gamma_{\text{ext}}$ decreases initially with a growth of γ_{ext} but, after reaching minimum value for $\gamma_{\text{ext}} \approx 40°$, it starts to grow again. The theoretical dependencies of the external angles $\theta_{o,\text{ext}}$ and $\theta_{e,\text{ext}}$ on γ_{ext} [Fig. 4(b)] are in very good agreement with the experimental results [Fig. 4(a)].

Although the period of the poled grating does not appear in Eqs. (2), the LPM signals are not visible in experiments with single-domain crystals. On the other hand, if both TPM and LPM are satisfied simultaneously (the case of nonlinear Bragg diffraction [3]), the respective diffraction order is much more intense than the neighboring SH diffraction spots.

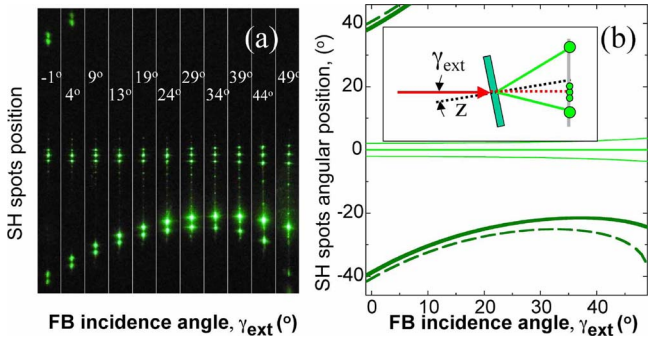

Fig. 4. (Color online) (a) Positions of the SH diffraction spots versus γ_{ext}, measured on a screen perpendicular to the FF beam. (b) Theoretical prediction. Central curves, TPM-SH; thick curves, LPM-SH. E_2–O_1O_1, solid thick curve; O_2–O_1O_1, dashed thick curve. Inset, scheme of the angle-dependence experiment.

In conclusion, we have observed second-harmonic patterns generated owing to multiorder nonlinear diffraction. We have found that the angular positions of the SH beams are defined only by the ratio of the wavelength to the grating period as in Raman–Nath diffraction in linear optics. The diffraction patterns include additional spots defined only by the longitudinal phase matching, not being observable without the nonlinear grating. For this reason we believe these peripheral SH spots can be identified as a noninteger order nonlinear diffraction. As recently shown [16], similar type SH radiation can be used for single-shot reconstruction of femtosecond pulses. The observed phenomena can also find application in nonlinear microscopy and nondestructive evaluation of the domain structure in ferroelectric crystals.

This work was supported by the Australian Research Council and Israeli Science Foundation. S. Saltiel acknowledges the Nonlinear Physics Centre for hospitality and support.

References

1. M. M. Fejer, G. A. Magel, D. H. Jundt, and R. L. Byer, IEEE J. Quantum Electron. **QE-28**, 2631 (1992).
2. M. Born and E. Wolf, *Principles of Optics* (Cambridge U. Press, 1999), Chap. 12.
3. I. Freund, Phys. Rev. Lett. **21**, 1404 (1968).
4. G. Dolino, Phys. Rev. B **6**, 4025 (1972).
5. Y. Le Grand, D. Rouede, C. Odin, R. Aubry, and S. Mattauch, Opt. Commun. **200**, 249 (2001).
6. A. L. Aleksandrovskii and V. V. Volkov, Quantum Electron. **26**, 542 (1996).
7. A. Apostoluk, D. Chapron, G. Gadret, B. Sahraoui, J. Nunzi, C. Fiorini-Debuisschert, and P. Raimond, Opt. Lett. **27**, 2028 (2002).
8. S. Moscovich, A. Arie, R. Urneski, A. Agronin, G. Rosenman, and Y. Rosenwaks, Opt. Express **12**, 2236 (2004).
9. I. V. Shutov, I. A. Ozheredov, A. V. Shumitski, and A. S. Chirkin, Opt. Spectrosc. **105**, 79 (2008).
10. S. Saltiel, D. Neshev, W. Krolikowski, R. Fischer, A. Arie, and Yu. Kivshar, Phys. Rev. Lett. **100**, 103902 (2008).
11. A. Fragemann, V. Pasiskevicius, and F. Laurell, Appl. Phys. Lett. **85**, 375 (2004).
12. A. A. Kaminskii, H. Nishioka, K. Ueda, W. Odajima, M. Tateno, K. Sasaki, and A. V. Butashin, Quantum Electron. **26**, 381 (1996).
13. A. R. Tunyagi, M. Ulex, and K. Betzler, Phys. Rev. Lett. **90**, 243901 (2003).
14. R. Fischer, D. N. Neshev, S. M. Saltiel, W. Krolikowski, and Yu. S. Kivshar, Appl. Phys. Lett. **89**, 191105 (2006).
15. A. S. Aleksandrovsky, A. M. Vyunishev, A. I. Zaitsev, A. V. Zamkov, and V. G. Arkhipekin, J. Opt. A **16**, S334 (2007).
16. S. J. Holmgren, C. Canalias, and V. Pasiskevicius, Opt. Lett. **32**, 1545 (2007).